ATMOSPHERIC SCIENCE

Atmospheric rivers drive flood damages in the western United States

Thomas W. Corringham[1]*, F. Martin Ralph[1], Alexander Gershunov[1], Daniel R. Cayan[1], Cary A. Talbot[2]

Atmospheric rivers (ARs) are extratropical storms that produce extreme precipitation on the west coasts of the world's major landmasses. In the United States, ARs cause significant flooding, yet their economic impacts have not been quantified. Here, using 40 years of data from the National Flood Insurance Program, we show that ARs are the primary drivers of flood damages in the western United States. Using a recently developed AR scale, which varies from category 1 to 5, we find that flood damages increase exponentially with AR intensity and duration: Each increase in category corresponds to a roughly 10-fold increase in damages. Category 4 and 5 ARs cause median damages in the tens and hundreds of millions of dollars, respectively. Rising population, increased development, and climate change are expected to worsen the risk of AR-driven flood damage in future decades.

INTRODUCTION

Atmospheric rivers (ARs) are temporally ephemeral filamentary features in the lower troposphere that horizontally transport large quantities of water vapor (on average, more than double the flow of the Amazon River) and can cause extreme precipitation events on west coasts of major landmasses due to orographic lift over mountainous topography (*1*). Since their early characterization in 1998 using weather model data (*2*), satellite and aircraft observations confirmed the modeling study (*3*) and documented their role in causing significant floods (*4*). ARs have since been shown to be an important source of intraseasonal and interannual variations in precipitation and streamflow in the western United States and globally (*5*, *6*). There is a growing awareness that ARs are responsible for a wide range of environmental, social, and economic impacts, affecting the frequency and severity of extreme floods and influencing drought duration and intensity (*7*). ARs have been identified as the primary source of hydrologic flooding in the western United States (*8*, *9*), yet their costs remain largely unquantified. Since sea surface temperature near the coast is a determinant of the amount of rain associated with an AR (*10*), quantifying the relationship between AR intensity and economic impact is important, given the rising ocean-atmosphere heat content associated with climate change.

On 4 January 1995, a strong AR developed off the coast of California (Fig. 1A). A plume of precipitable water vapor extended from Hawaii to the west coast of North America. At the coast, integrated vapor transport (IVT) was greater than 712 kg m^{-1} s^{-1}. By 9 January, coastal IVT reached 966 kg m^{-1} s^{-1}, producing extreme precipitation in Sonoma County, California, which then caused streamflow to peak in the lower reach of the Russian River at Guerneville (Fig. 1B). The river rose above flood stage for 7 days. Insured losses in Sonoma County totaled over $50 million over a 3-day period as the town of Guerneville was inundated (Fig. 1C). Impacts were widespread in central California; in terms of insured losses, this was the most damaging event in the 40-year record in the western United States and is 1 of the 11 ARs that caused over $1 billion in total estimated damages (Table 1).

Catastrophic scenarios have been modeled in detail: The ARkStorm scenario (*11*) simulated an approximately 1-in-1000-year series of ARs, estimating damages of up to $840 billion (all values in 2018 dollars), but did not quantify the effects of more frequent, lower-intensity flood events. While cost estimates for individual flood events are often available (*12*, *13*), cost estimation methods are generally not consistent across events. Here, we combine spatially and temporally consistent flood insurance loss data from the National Flood Insurance Program (NFIP) with measures of total damages from a National Weather Service (NWS) dataset (*14*) and a complete catalog of west coast ARs (*10*) to provide a comprehensive analysis of flood damages caused by ARs in the western United States over the past 40 years.

RESULTS

Across the 11 western conterminous states, from 1978 to 2017, we find that total estimated flood damages, during all seasons, amounted to $50.8 billion, and ARs accounted for 84% of these damages, i.e., $42.6 billion, or roughly $1.1 billion a year. In this study, AR activity is identified by daily maximum 6-hour vertically IVT greater than 250 kg m^{-1} s^{-1}, over a string of coastal 2.5° grid cells (fig. S1), meeting additional geometric and temporal conditions (*10*). Over the sample period, 1603 separate ARs made landfall from 27.5°N in Baja California to 47.5°N in Washington. AR total estimated damages are defined as NFIP-insured losses occurring anywhere in the western United States on the day of or the day following AR conditions, inflated by a factor of 30, which was determined by Corringham and Cayan (*15*) in an analysis of NFIP-insured losses against an NWS dataset (*14*) of total damages by state by year over a 21-year period for which both datasets were available (fig. S2). The NWS data (*14*) are based on information from newspapers; estimates from emergency managers, insurance agents, and local officials; damage assessments by Federal Emergency Management Agency (FEMA) storm survey teams; and crop damage estimates from the U.S. Department of Agriculture. Insurance data were obtained directly from the NFIP.

In the coastal states of California, Oregon, and Washington, the proportions of total insured flood damages attributable to ARs exceeded 99% in some areas (Fig. 2 and Table 2). Relatively high proportions of damages were associated with AR activity as far east as 100°W, including much of Arizona, Idaho, and western Montana—inland regions where ARs are known to penetrate (*16*). Damages in

[1]Center for Western Weather and Water Extremes (CW3E), Scripps Institution of Oceanography, University of California San Diego, La Jolla, CA, USA. [2]U.S. Army Corps of Engineers, Engineer Research and Development Center, Vicksburg, MS, USA. *Corresponding author. Email: tcorringham@ucsd.edu

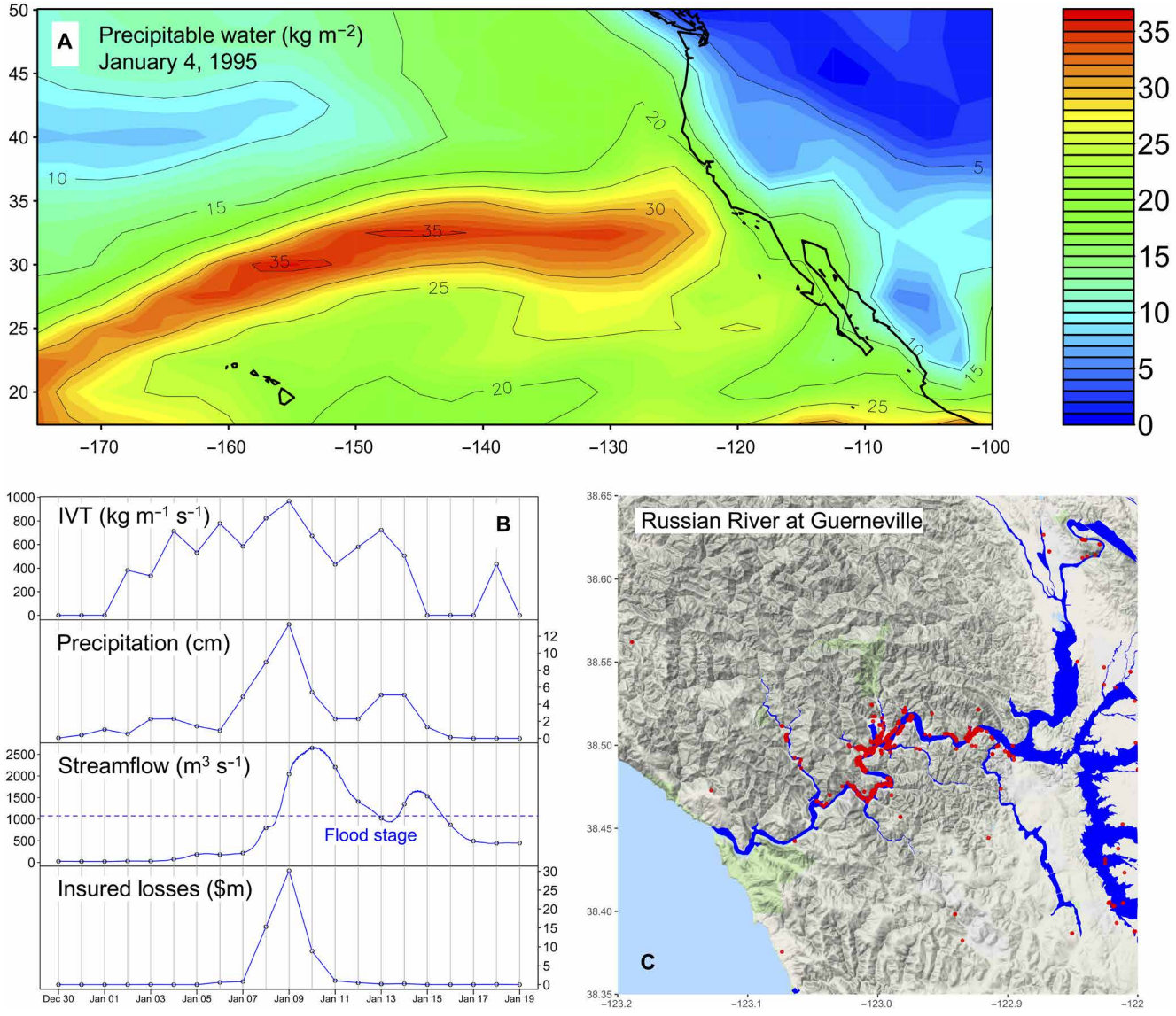

Fig. 1. An AR on 9 January 1995 caused substantial damages on the west coast of the United States. (**A**) 4 National Center of Environmental Prediction–National Center for Atmospheric Research (NCEP-NCAR) precipitable water preceded peak damages in California. (**B**) Maximum coastal IVT (given here over the entire west coast), generated peak precipitation over Sonoma County (see Materials and Methods), streamflow at the U.S. Geological Survey Guerneville gauge, and total insured losses in Sonoma County. (**C**) Flood insurance claims along the lower reach of the Russian River in Sonoma County are marked as red dots; the 100-year flood plain is indicated in blue.

Arizona were due to ARs making landfall in Baja California; damages in Idaho and Montana resulted from inland penetration of ARs through the Columbia River Valley, indicating the importance of the orientation of ARs relative to topography in generating damaging floods (*17*). Causes of flood damages in the western United States other than ARs included remnant tropical storms, cutoff low-pressure systems, the North American monsoon, and mesoscale convective systems (*18*). These mechanisms resulted in highly damaging events, but their combined impact across the West was surpassed fivefold by the effect of ARs.

Flood damages have been concentrated spatially and temporally. The top 20 counties of the 414 counties of the western United States accounted for 69% of flood damages over the sample period (Table 2). In these counties, large fractions of damages were associated with AR activity. Proportions were over 0.99 in Sonoma County, which experienced the highest damages of the counties over the sample period and is located at the peak of AR land-falling activity along the west coast, in terms of ARs of all intensities [(*10*), see also (*19*)]. The most affected areas were typically not the most densely populated regions in the western United States, but those with vulnerable assets located near rivers or coastlines prone to significant flooding. Slightly lower but still high proportions of total damages caused by ARs (82 to 95%) were observed in southern California and the interior Southwest (Fig. 2 and Table 2).

A small number of extreme and exceptional ARs were responsible for a large proportion of total flood damages over the sample period (Fig. 3A and fig. S3A). Only 13 events, spanning 65 days, caused over $1 billion in estimated total damages (Table 1). These events accounted for 58.3% of total insured losses in the sample. These highly damaging ARs were multiday events varying in length from

Table 1. Most damaging atmospheric rivers 1978–2017.

Start date	Initial landfall region	Initial landfall latitude	AR category	Peak IVT (kg m^{-1} s^{-1})	Claims	Insured losses ($m)	Total damages ($b)
4 January 1995	S. CA	32.5°N	4	966	4725	125.8	3.7
29 December 2005	N. CA	40°N	4	825	2554	117.6	3.5
29 December 1996	Central CA	35°N	5	1260	3407	104.6	3.1
5 February 1996	N. OR	45°N	3	729	2695	99.3	3.0
2 December 2007	N. OR	45°N	5	1258	1447	83.9	2.5
15 February 1986	WA	47.5°N	4	870	2048	66.6	2.0
7 March 1995	S. OR	42.5°N	4	928	2343	58.7	1.8
5 January 2009	S. OR	42.5°N	4	831	1636	53.9	1.6
1 February 1998	Bay Area	37.5°N	4	795	2417	46.8	1.4
1 November 2006	N. CA	40°N	5	1041	1184	38.7	1.2
25 January 1983	Bay Area	37.5°N	5	1013	1545	34.9	1.0
25 February 1983	Bay Area	37.5°N	3	658	1832	30.0	0.9
12 February 1980	Baja CA	30°N	3	721	2059	28.5	0.9
3 January 1982	N. CA	40°N	3	525	1422	28.1	0.8
11 February 1986	N. CA	40°N	4	904	848	23.9	0.7
21 November 1990	WA	47.5°N	4	943	939	23.3	0.7

3 to 11 days, with peak damages generally occurring 1 day after initial landfall (fig. S3C). Spatially, the initial crossing latitude ranged from Baja California Norte to Washington, although over the course of many of these multiday events, the storm position over time varied widely from the initial landfall region. The mean orientation of ARs at all latitudes was southwest to northeast, with damages typically occurring to the northeast of landfall (fig. S4). Values of AR intensity as measured by maximum IVT over the course of the events were uniformly high. In most of these highly damaging events, peak IVT was over 750 kg m^{-1} s^{-1}. The highly impactful New Year's flood of 1996–1997 experienced a very rare exceptional peak IVT of 1260 kg m^{-1} s^{-1}.

A recently developed scale of AR intensity (*20*) similar to scales for hurricanes and tornadoes (*21*, *22*) captures a range of AR effects, classifying ARs from category 1 to 5. The scheme (Fig. 3A) categorizes ARs based on peak IVT in increments of 250 kg m^{-1} s^{-1} and then adjusts the category based on the duration of the event. Although some ARs cause significant damage, most are largely beneficial. ARs are known to generate much of the annual precipitation in California and the western United States, replenishing the region's water supply (*7*), and the insurance record reveals that about half (801) of all ARs in the sample caused no insured losses.

Effects of ARs by category are posited to range from mostly beneficial (categories 1 and 2: short duration, low IVT) to mostly damaging (categories 4 and 5: long duration, high IVT). An examination of November to March (NDJFM) flood damages supports these assertions (Fig. 3B and Table 3). Category 1 and 2 storms caused negligible median damages of under $1 million, while category 4 and 5 storms caused significant median damages in the tens and hundreds of millions of dollars over the study period of 1978 to 2017 during the AR damage season (NDJFM). Notably, with each increase in AR category, 2 and above, median damages increased roughly by an order of magnitude: Increases in AR duration and intensity led to exponential increases in flood damages.

While the AR scale corresponds well to insured flood losses and estimated total damages, there was significant variability in damages within each category. Beyond peak IVT and duration, several other factors were important determinants of AR-related flood damages. For example, the two least damaging category 5 storms (11 November 1983 at 42.5°N and 29 November 2007 at 27.5°N) affected sparsely populated areas early in the wet season when soils were still dry and able to absorb most of the extreme precipitation, causing less than $10 million in damages. In contrast, the most damaging category 1 storm occurred 2 weeks after the devastating 1996–1997 New Year's flood in northern California and western Nevada when soils and snowpack were primed for high runoff and river stages were already at high levels (*23*), causing over $200 million in damages.

Evidence for the importance of antecedent hydrologic conditions is found in the annual timing of damages relative to AR activity (fig. S5 and table S1). Peak levels of IVT over the western coastal regions occurred from October to February, as AR land-falling activity progressed down the coast, peaking in fall in the Pacific Northwest and in winter in California (*10*, *19*). Over the course of the water year, mean damages lagged AR activity by 1 month: The AR damage season occurred from November to March. Mean levels of IVT were lowest in the summer months, as were damages. During winter months, ARs that occurred in succession caused considerably more damage than isolated events: Mean damages of NDJFM ARs increased significantly when category 4 or 5 ARs occurred within the previous 5 or 10 days (table S2).

Another key determinant of the economic impact of strong to exceptional ARs is the location of AR landfall relative to assets at risk. The number of flood insurance policies in a given area is a good proxy

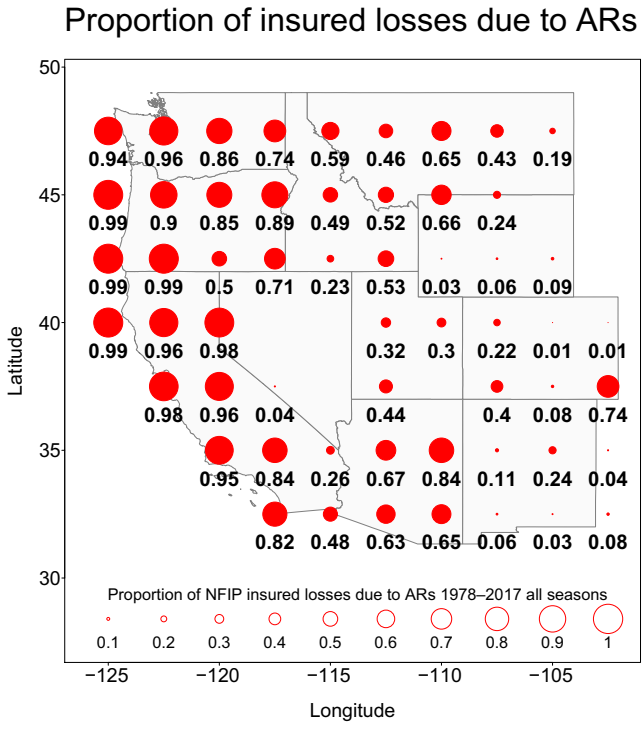

Fig. 2. From 1978 to 2017, ARs accounted for 84.2% of all insured flood losses in the 11 western states across all seasons. In many areas in coastal northern California and the Pacific Northwest, ARs accounted for over 95% of insured flood losses.

for exposure (tables S3 and S4), but the specific locations of vulnerable assets are also important, as in the January 1995 Guerneville event described above. Total damages may also depend critically on infrastructure. On 7 February 2017, following months of record-breaking cumulative precipitation, a category 4 AR damaged the main and emergency spillways of the Oroville Dam in northern California, causing the evacuation of over 180,000 residents and over $1 billion in damages (*20*, *24*, *25*).

DISCUSSION

In a warmer climate, extreme ARs will become more intense (*26*) as they become wetter, longer, and wider (*27*); there is some indication that this is already happening in association with observed Pacific Ocean warming (*10*). ARs are projected to increasingly dominate the region's changing hydroclimate with its increasingly volatile precipitation regime (*28*, *29*). We have shown that modest increases in AR intensity could lead to significant increases in damages. The increase in exposure to risk over the coming decades, as population in the western coastal states continues to grow (*30*), is likely to drive damages even higher.

Many communities in the western United States have been repeatedly affected by catastrophic floods. In addition to hardening flood control infrastructure (*31*), there have long been calls for the federal government to buy back high-risk properties rather than encourage residents to rebuild in flood hazard areas through the provision of subsidized flood insurance (*32*). Moreover, the traditional quantification of economic impacts associated with flooding often

Table 2. Proportion of losses caused by ARs in top counties.

County	AR proportion of insured losses	Claims	Insured losses ($m)	Total damages ($b)	AR damages ($b)
Sonoma, CA	0.998	6650	172.0	5.2	5.2
Los Angeles, CA	0.846	8280	106.1	3.2	2.7
Lewis, WA	0.989	1979	101.4	3.0	3.0
Marin, CA	0.987	3152	73.2	2.2	2.2
King, WA	0.970	2915	69.0	2.1	2.0
Sacramento, CA	0.977	3609	56.9	1.7	1.7
Snohomish, WA	0.903	1818	43.7	1.3	1.2
Monterey, CA	0.989	1253	43.5	1.3	1.3
Napa, CA	0.997	1331	43.2	1.3	1.3
Washoe, NV	0.998	720	42.4	1.3	1.3
Maricopa, AZ	0.628	2368	33.7	1.0	0.6
Santa Clara, CA	0.971	1557	33.4	1.0	1.0
Clackamas, OR	0.970	730	31.5	0.9	0.9
San Diego, CA	0.912	1945	30.7	0.9	0.8
Orange, CA	0.899	3619	29.3	0.9	0.8
Pierce, WA	0.974	934	28.4	0.9	0.9
Riverside, CA	0.624	1619	27.9	0.8	0.5
Cowlitz, WA	0.596	709	26.6	0.8	0.5
Placer, CA	0.990	598	26.5	0.8	0.8
Columbia, OR	0.998	414	24.7	0.7	0.7

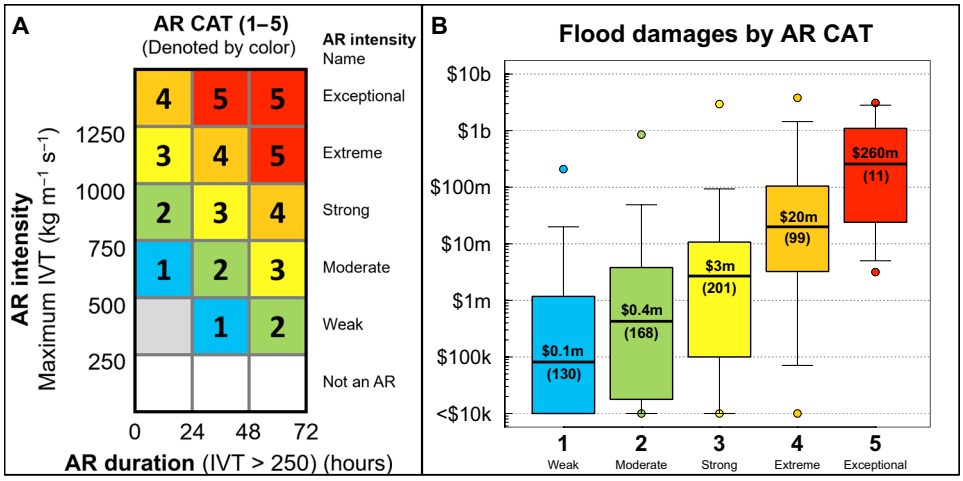

Fig. 3. Flood damages increase exponentially with AR category. (**A**) The Ralph *et al.* AR scale (*20*) classifies ARs into five categories depending on IVT and duration. For example, an AR with a peak IVT of 800 kg m^{-1} s^{-1} and a duration of 78 hours is classified as a category 4 or extreme AR. (**B**) NDJFM flood damages increase exponentially with AR category: Vertical scale is logarithmic; black bars are medians; boxes are 25th and 75th percentiles, and whiskers are 5th and 95th percentiles; dots are extrema; numbers in parentheses are the number of NDJFM events in each category. Note that the total number of ARs in the Gershunov AR catalog (1603) is greater than the number of ARs over the sample period using the Ralph *et al.* AR scale (1134), which classifies events with a duration of less than 24 hours as non-ARs.

Table 3. Summary statistics of damages by atmospheric river category, November to March, in millions of dollars. Damages under $50,000 are rounded down to $0.

AR CAT	Number of events	Minimum ($m)	5% ($m)	25% ($m)	Median ($m)	75% ($m)	95% ($m)	Maximum ($m)
CAT 1	130	0	0	0	0.1	1	24	208
CAT 2	168	0	0	0	0.3	4	48	844
CAT 3	201	0	0	0.1	2	10	94	2930
CAT 4	99	0	0.1	3	19	85	1424	3773
CAT 5	11	3	5	24	259	1102	2821	3126
All ARs	609	0	0	0	2	10	197	3773

neglects ecological impacts. There is a growing recognition that in addition to conventional large-scale flood control infrastructure, policymakers must also consider nonstructural flood damage mitigation approaches, including the restoration of natural flood plains and the strategic placement of green infrastructure (*33*). As ARs increase in intensity, bolstering extreme precipitation over the coming decades (*26*, *34*), the case for these policy changes is strengthened.

Improved prediction of AR frequency and intensity, as well as latitude of landfall and duration of individual AR events, in near-term and at subseasonal-to-seasonal time scales could provide significant increases in the efficiency of water operations at reservoirs by achieving simultaneous improvements in both water conservation and flood management through forecast-informed reservoir operations. These improvements could be realized without costly and time-consuming structural modifications. Benefits to emergency management officials could also be realized through more effective prepositioning of resources and use of evacuation measures. To help focus future research and forecasting improvements, we recommend that the National Oceanic and Atmospheric Administration begin tracking damages by ARs, as they have long done for hurricanes and tornadoes.

MATERIALS AND METHODS

Economic data and methods

NFIP loss data comprise daily claims from 1978 to 2017, with each claim located to the nearest NFIP community (city, typically, or county remainder) and listing the total insured loss to the building and its contents by claim. All monetary values were adjusted for inflation to 2018 U.S. dollars (*35*). A comparison of 1983 to 2003 annual NFIP losses to an NWS compilation of economic impacts of flooding (fig. S2) (*14*) established that insured losses are a good proxy for overall economic impacts. The NWS data comprise annual total estimated damages due to flooding at the state level from 1983 to 2003, as reported by newspaper articles and the reports of federal agencies.

In the 11 western states, NFIP-insured losses account for roughly $^1/_{30}$ of total damages as estimated by the NWS; the Pearson correlation between the two time series is 0.8. In this study, the 30-fold difference between insured losses and total impacts was used to provide an estimate of total economic impacts associated with flood events. Given the low spatial and temporal resolution of the NWS data, the total damage estimates are highly imprecise. The measures of insured flood losses, on the other hand, are exact and easily comparable over space and time.

Although the NFIP data have several attractive features, they also suffer from significant limitations. Participation rates are low in the western United States (*36*), even in relatively high-risk areas, so the numbers of claims and insured losses are imperfect measures of total damages. Several biases are expected. Floods in unexpected areas will be underrepresented. The NFIP program covers only residential property, so floods that cause disproportionate damage to agriculture, infrastructure, and industrial plants will be down-weighted in this analysis. Older properties receive subsidies and are likely overrepresented in the portfolio of risks. This is one of many distortions in the NFIP. The market for insurance is not a free market and does not behave like one (*37*). These caveats aside, the NFIP data are highly resolved temporally and spatially specific, so they provide a useful source with which to assess the economic impacts of flood events associated with ARs and extreme hydrologic events more generally.

As of policy year 2017, there were approximately 392,000 policyholders in the 1807 participating NFIP communities in the 11 western states. The total coverage in force was $118 billion. Total premiums paid in were $292 million, or 0.247% of total coverage in force. The average policyholder paid an annual premium of $745 for $301,000 coverage. Further summary statistics of the NFIP data are given in (*15*). To analyze the impacts of ARs on insured losses, NFIP loss data and total damage estimates were aggregated spatially over a 2.5° grid (Fig. 2) and by county (fig. S4 and Table 2). Daily claims and insured losses were used throughout, with days defined in local time for the NFIP dataset.

AR data and methods

AR data were obtained from Gershunov *et al.* (G17) (*10*), who present an AR detection methodology through which they compile a comprehensive catalog of ARs over 70 years using National Center of Environmental Prediction–National Center for Atmospheric Research (NCEP-NCAR) reanalysis. The G17 catalog was chosen because of its long duration, its focus on the western United States, and its comparison with independent high-resolution daily precipitation observations; cf. (*6*, *16*, *38*, *39*) for other AR detection methodologies.

The G17 catalog identifies the ARs that make landfall along the Pacific coast of North America over a 2.5° coastal grid. ARs identified were those events whose 6-hour average vertically integrated horizontal vapor transport (IVT) exceeded 250 kg s^{-1} m^{-1}, along with exceeding prescribed vertically integrated specific humidity and conforming to certain geometric requirements. In addition to time and place of AR occurrences, G17 also provides the zonal and meridional components of IVT and wind at 850 hPa over a 2.5° grid of the north Pacific and the western United States at a 6-hour time scale. These data were aggregated to daily resolution in local time using mean and maximal values of the variables by grid cell. If a 6-hour period in a day in local time reached the AR IVT threshold, then it was considered an AR day for this study. This allows direct comparison with daily NFIP flood claims from 1978 to 2017.

Inspection of a number of individual damaging ARs led to a concern that the low spatial resolution of the NCEP-NCAR reanalysis data generated maximum IVT values that were lower than expected, so maximum IVT values were bias-corrected using a comparison to more recent NASA Modern-Era Retrospective analysis for Research and Applications, Version 2 data. Following results reported in table 2 of Ralph *et al.* (*38*), IVT values were increased by 44 kg m^{-1} s^{-1} in the G17 (*10*) data before the Ralph *et al.* AR classification scheme (*20*) was applied.

In the G17 data, there were 1603 events in the 1978–2017 sample (40 per year on average). The durations of daily aggregated events in the sample ranged from 6 hours to 16 days. Median AR duration was 30 hours; mean duration was 40 hours. ARs making landfall from 27.5°N to 47.5°N, that is, over nine 2.5° latitude bands, are considered (fig. S1). During the course of a multiday event, an AR may make landfall at more than one latitude band. In the sample, ARs were observed making landfall at one to nine separate 2.5° latitude bands over the course of the event. The mean number of land-falling latitude bands per event was 2.65. The median and modal number of latitude bands was two. The nine coastal grid cells, with arrows indicating the mean IVT direction at landfall, are indicated in fig. S1.

January 1995 event data and methods

North Pacific precipitable water (kg m^{-2}) was obtained from NCEP-NCAR reanalysis and averaged over four 6-hour time periods [Coordinated Universal Time (UTC)] on 4 January 1995. IVT values (kg m^{-1} s^{-1}) are maximum values for the west coast from 27.5°N to 47.5°N (note that IVT at 37.5°N has gaps where IVT falls below the 250 kg m^{-1} s^{-1} threshold over the 11-day time period). Precipitation (in millimeters) was derived by taking the maximum value of precipitation over $^1/_8$-degree gridded Livneh *et al.* (*40*) data over Sonoma County. Streamflow was obtained from the United States Geological Survey (USGS) at the Guerneville gauge (11467000) at 15-min resolution and converted from cubic feet per second to cubic meters per second. Insured losses are NFIP losses aggregated over Sonoma County. Mapped flood insurance claim locations were taken from an NFIP claims dataset. The 100-year flood plain (FEMA Special Flood Hazard Area) polygons were derived from NFIP Q3 digitized flood plain maps. Topography was derived from Google Maps (2018).

ARs and insured losses

The G17 AR catalog was matched to NFIP claims and insured losses to calculate the proportion of ARs that caused insured losses and the mean insured loss per event. From this, total direct economic damages were estimated using the relationship between NFIP losses and NWS-reported damages. To calculate the proportion of insured losses attributable to ARs, insured losses on days with a maximum IVT of >250 kg m^{-1} s^{-1}, or the following day, observed in at least one of the nine coastal grid cells (fig. S1) were divided by insured losses on all days in the sample, using loss data aggregated by a 2.5° grid cell (Fig. 2) or by county (Table 2).

SUPPLEMENTARY MATERIALS

Supplementary material for this article is available at http://advances.sciencemag.org/cgi/content/full/5/12/eaax4631/DC1

Supplementary Text
Fig. S1. Coastal grid cells.
Fig. S2. NFIP payments versus NWS damages.
Fig. S3. Distribution and time course of insured losses.
Fig. S4. Spatial footprints of ARs.
Fig. S5. Seasonality of insured losses.
Fig. S6. Days with over $1 million in insured losses.
Table S1. Damages by AR category by month, in millions of dollars.
Table S2. Effect of antecedent ARs on mean flood damages by AR event.
Table S3. Average claims and insured losses per latitude-day by AR intensity (quartiles).
Table S4. Daily average insured losses by latitude band by AR intensity.
Data S1.
Reference (*41*)

REFERENCES AND NOTES

1. American Meteorological Society, *Glossary of Meteorology* (2017).
2. Y. Zhu, R. E. Newell, A proposed algorithm for moisture fluxes from atmospheric rivers. *Mon. Wea. Rev.* **126**, 725–735 (1998).

3. F. M. Ralph, P. J. Neiman, G. A. Wick, Satellite and CALJET aircraft observations of atmospheric rivers over the eastern North Pacific Ocean during the winter of 1997/98. *Mon. Wea. Rev.* **132**, 1721–1745 (2004).
4. F. M. Ralph, P. J. Neiman, G. A. Wick, S. I. Gutman, M. D. Dettinger, D. R. Cayan, A. B. White, Flooding on California's Russian river: Role of atmospheric rivers. *Geophys. Res. Lett.* **33**, L13801 (2006).
5. M. D. Dettinger, F. M. Ralph, T. Das, P. J. Neiman, D. R. Cayan, Atmospheric rivers, floods and the water resources of California. *Water* **3**, 445–478 (2011).
6. B. Guan, D. E. Waliser, Detection of atmospheric rivers: Evaluation and application of an algorithm for global studies. *J. Geophys. Res. Atmos.* **120**, 12514–12535 (2015).
7. M. D. Dettinger, Atmospheric rivers as drought busters on the U.S. West Coast. *J. Hydrometeorol.* **14**, 1721–1732 (2013).
8. N. A. Barth, G. Villarini, M. A. Nayak, K. White, Mixed populations and annual flood frequency estimates in the western United States: The role of atmospheric rivers. *Water Resour. Res.* **53**, 257–269 (2017).
9. C. P. Konrad, M. D. Dettinger, Flood runoff in relation to water vapor transport by atmospheric rivers over the western United States, 1949–2015. *Geophys. Res. Lett.* **44**, 11,456–11,462 (2017).
10. A. Gershunov, T. Shulgina, F. M. Ralph, D. A. Lavers, J. J. Rutz, Assessing the climate-scale variability of atmospheric rivers affecting western North America. *Geophys. Res. Lett.* **44**, 7900–7908 (2017).
11. K. Porter, A. Wein, C. Alpers, A. Baez, P. Barnard, J. Carter, A. Corsi, J. Costner, D. Cox, T. Das, M. Dettinger, J. Done, C. Eadie, M. Eymann, J. Ferris, P. Gunturi, M. Hughes, R. Jarrett, L. Johnson, H. D. Le-Griffin, D. Mitchell, S. Morman, P. Neiman, A. Olsen, S. Perry, G. Plumlee, M. Ralph, D. Reynolds, A. Rose, K. Schaefer, J. Serakos, W. Siembieda, J. Stock, D. Strong, I. S. Wing, A. Tang, P. Thomas, K. Topping, C. Wills, L. Jones, "Overview of the ARkStorm scenario" (Tech. Rep., USGS 2010–1312, 2011).
12. California Department of Water Resources, "California's Flood Future: Recommendations For Managing The State's Flood Risk" (Tech. Rep. 2013).
13. F. Dominguez, S. Dall'erba, S. Huang, A. Avelino, A. Mehran, H. Hu, A. Schmidt, L. Schick, D. Lettenmaier, Tracking an atmospheric river in a warmer climate: From water vapor to economic impacts. *Earth Syst. Dynam.* **9**, 249–266 (2018).
14. M. W. Downton, J. Z. Barnard Miller, R. A. Pielke Jr., Reanalysis of U.S. national weather service flood loss database. *Nat. Haz. Rev.* **6**, 13–22 (2005).
15. T. W. Corringham, D. R. Cayan, The effect of El Niño on flood damages in the western United States. *Wea. Climate Soc.* **11**, 489–504 (2019).
16. J. J. Rutz, W. J. Steenburgh, F. M. Ralph, Climatological characteristics of atmospheric rivers and their inland penetration over the western United States. *Mon. Wea. Rev.* **142**, 905–921 (2014).
17. K. A. Guirguis, A. Gershunov, T. M. Shulgina, R. E. S. Clemesha, F. M. Ralph, Atmospheric rivers impacting Northern California and their modulation by a variable climate. *Clim. Dyn.* **52**, 6569–6583 (2019).
18. K. K. Hirschboeck, "Hydrology of Floods and Droughts, Climate and Floods" (USGS Water Supply Paper 237, 1991).
19. M. D. Dettinger, F. M. Ralph, J. J. Rutz, Empirical return periods of the most intense vapor transports during historical atmospheric river landfalls on the U.S. West Coast. *J. Hydrometeorol.* **19**, 1363–1377 (2018).
20. F. M. Ralph, J. J. Rutz, J. M. Cordeira, M. Dettinger, M. Anderson, D. Reynolds, L. J. Schick, C. Smallcomb, A scale to characterize the strength and impacts of atmospheric rivers. *Bull. Amer. Meteor. Soc.* **100**, 269–289 (2019).
21. Weatherwise, The hurricane disaster—Potential scale. 27, 169–186 (1974).
22. T. T. Fujita, "Proposed Characterization of Tornadoes and Hurricanes by Area and Intensity" (Tech. Rep. SMRP 91, University of Chicago, 1971).
23. S. E. Hammond, J. G. Harmon, "Publications Document Floods of January 1997 in California and Nevada" (USGS Fact Sheet FS-093-98, 1998).
24. J. A. Vano, K. Miller, M. D. Dettinger, R. Cifelli, D. Curtis, A. Dufour, J. R. Olsen, A. M. Wilson, Hydroclimatic extremes as challenges for the water management community: Lessons from Oroville Dam and hurricane harvey. *Bull. Amer. Meteor. Soc.* **100**, S9–S14 (2019).
25. A. B. White, B. J. Moore, D. J. Gottas, P. J. Neiman, Winter storm conditions leading to excessive runoff above California's Oroville Dam during January and February 2017. *Bull. Amer. Meteor. Soc.* **100**, 55–70 (2019).
26. A. Gershunov, T. Shulgina, R. E. S. Clemesha, K. Guirguis, D. W. Pierce, M. D. Dettinger, D. A. Lavers, D. R. Cayan, S. D. Polade, J. Kalansky, F. M. Ralph, Precipitation regime change in Western North America: The role of Atmospheric Rivers. *Sci. Rep.* **9**, 9944 (2019).
27. V. Espinoza, D. E. Waliser, B. Guan, D. A. Lavers, F. M. Ralph, Global analysis of climate change projection effects on atmospheric rivers. *Geophys. Res. Lett.* **45**, 4299–4308 (2018).
28. S. D. Polade, A. Gershunov, D. R. Cayan, M. D. Dettinger, D. W. Pierce, Precipitation in a warming world: Assessing projected hydro-climate changes in California and other Mediterranean climate regions. *Sci. Rep.* **7**, 10783 (2017).
29. D. L. Swain, B. Langenbrunner, J. D. Neelin, A. Hall, Increasing precipitation volatility in twenty-first-century California. *Nat. Clim. Change* **8**, 427–433 (2018).
30. AECOM, Michael Baker Jr., Inc., Deloitte Consulting, LLP, "The impact of climate change and population growth on the National Flood Insurance Program through 2100" (Tech. Rep. AECOM, Michael Baker Jr., Inc., Deloitte Consulting, LLP, 2013).
31. National Research Council, *Disaster Resilience: A National Imperative* (The National Academies Press, 2012).
32. D. R. Conrad, B. McNitt, M. Stout, "Higher Ground" (Tech. Rep., National Wildlife Federation, 1998).
33. C. Kousky, S. M. Olmstead, M. A. Walls, M. Macauley, Strategically placing green infrastructure: Cost-effective land conservation in the floodplainp. *Environ. Sci. Technol.* **47**, 3563–3570 (2013).
34. D. A. Lavers, F. M. Ralph, D. E. Waliser, A. Gershunov, M. D. Dettinger, Climate change intensification of horizontal water vapor transport in CMIP5. *Geophys. Res. Lett.* **42**, 5617–5625 (2015).
35. U.S. Bureau of Economic Analysis, "Gross Domestic Product: Table 1.1.3. Real Gross Domestic Product, Quantity Indexes" (U.S. Bureau of Economic Analysis, 2018).
36. L. Dixon, N. Clancy, S. A. Seabury, A. Overton, "The National Flood Insurance Program's market penetration rate: Estimates and policy implications" (Tech. Rep., RAND Corporation, 2006).
37. E. O. Michel-Kerjan, Catastrophe economics: The national flood insurance program. *J. Econ. Perspectives* **24**, 165–186 (2010).
38. F. M. Ralph, A. M. Wilson, T. Shulgina, B. Kawzenuk, S. Sellars, J. J. Rutz, M. A. Lamjiri, E. A. Barnes, A. Gershunov, B. Guan, K. M. Nardi, T. Osborne, G. A. Wick, ARTMIP-early start comparison of atmospheric river detection tools: How many atmospheric rivers hit northern California's Russian River watershed? *Clim. Dynam.* **52**, 4973–4994 (2019).
39. C. A. Shields, J. J. Rutz, L.-Y. Leung, F. M. Ralph, M. Wehner, B. Kawzenuk, J. M. Lora, E. McClenny, T. Osborne, A. E. Payne, P. Ullrich, A. Gershunov, N. Goldenson, B. Guan, Y. Qian, A. M. Ramos, C. Sarangi, S. Sellars, I. Gorodetskaya, K. Kashinath, V. Kurlin, K. Mahoney, G. Muszynski, R. Pierce, A. C. Subramanian, R. Tome, D. Waliser, D. Walton, G. Wick, A. Wilson, D. Lavers; Prabhat, A. Collow, H. Krishnan, G. Magnusdottir, P. Nguyen, Atmospheric River Tracking Method Intercomparison Project (ARTMIP): Project goals and experimental design. *Geosci. Model Dev.* **11**, 2455–2474 (2018).
40. B. Livneh, E. A. Rosenberg, C. Lin, B. Nijssen, V. Mishra, K. M. Andreadis, E. P. Maurer, D. P. Lettenmaier, A long-term hydrologically based dataset of land surface fluxes and states for the conterminous United States: Update and extensions. *J. Climate* **26**, 9384–9392 (2013).
41. T. Cavazos, C. Turrent, D. P. Lettenmaier, Extreme precipitation trends associated with tropical cyclones in the core of the North American monsoon. *Geophys. Res. Lett.* **35**, L21703 (2008).

Acknowledgments: We thank T. M. Shulgina for assistance with the G17 dataset. **Funding:** The study is funded by the U.S. Bureau of Reclamation; the California-Nevada Climate Applications Program (CNAP), a National Oceanic and Atmospheric Administration Regional Integrated Sciences and Assessments team; the Southwest Climate Adaptation Science Center (SWCASC), a U.S. Geological Survey National Climate Adaptation Science Center; and the Multi-Campus Research Programs and Initiatives through the University of California Office of the President. **Author contributions:** T.W.C.: Data curation, formal analysis, investigation, methodology, visualization, and writing. A.G., D.R.C., and F.M.R.: Conceptualization, funding, methodology, supervision, and review and editing. C.A.T.: Review and editing. **Competing interests:** The authors declare that they have no competing interests. **Data and materials availability:** All data needed to evaluate the conclusions in the paper are present in the paper and/or the Supplementary Materials. Additional data related to this paper may be requested from the authors.

Submitted 25 March 2019
Accepted 18 September 2019
Published 4 December 2019
10.1126/sciadv.aax4631

Citation: T. W. Corringham, F. M. Ralph, A. Gershunov, D. R. Cayan, C. A. Talbot, Atmospheric rivers drive flood damages in the western United States. *Sci. Adv.* **5**, eaax4631 (2019).